Electronic Supplementary Material (ESI) for Nanoscale.

Supporting Information

Hybridized surface lattice modes in intercalated 3-disk plasmonic crystals for high figure-of-merit plasmonic sensing

*Landobasa Y M Tobing, Alana M Soehartono, Aaron D Mueller, Ken-Tye Yong, Wei Jun Fan, Dao Hua Zhang**

1. Possible combinations of constituent plasmonic crystals for 3-disk structures.

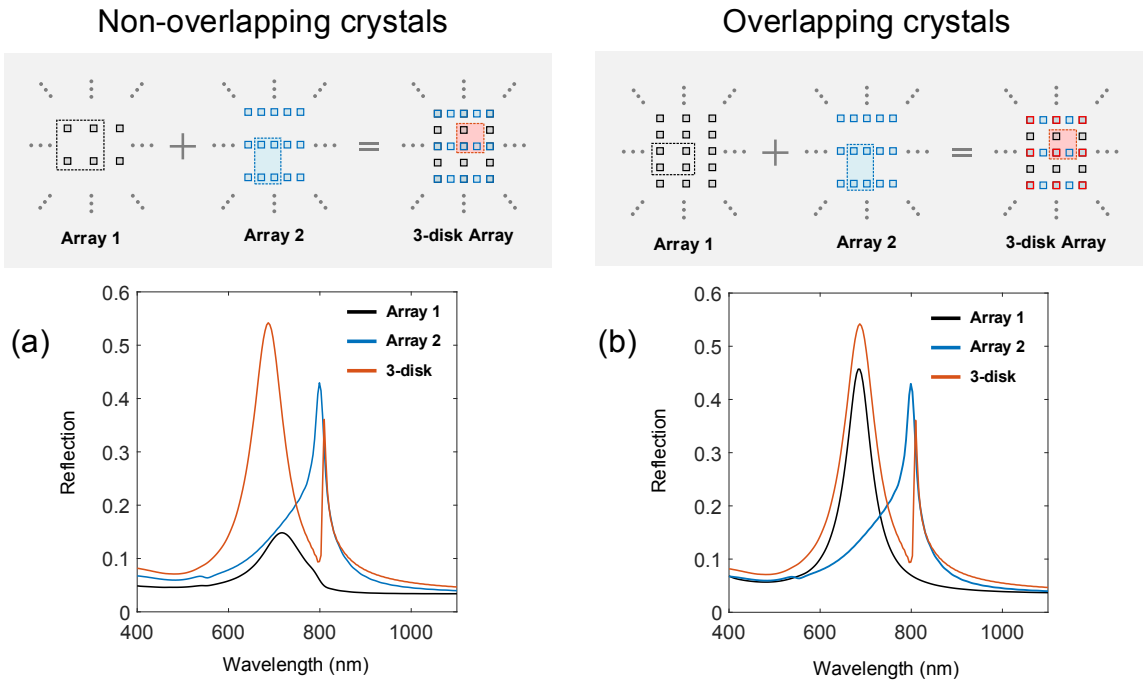

Figure S1. Possible combinations of constituent plasmonic crystals for the 3-disk structures. (a) Non-overlapping scheme, where Array 1 is the nanodisk array with both sparse periodicities in *x* and *y* directions. (b) Overlapping scheme, where Array 1 is the nanodisk array with a sparse periodicity in the *x* direction and a dense periodicity in the *y* direction. The Array 2 for both the non-overlapping and overlapping schemes are the same, which is the nanodisk array that is dense in the *x* direction and sparse in the *y* direction. The overlapping parts in the overlapping scheme are indicated by the red outlines.

2. Benchmarking with rectangular lattice plasmonic disk array and other structures

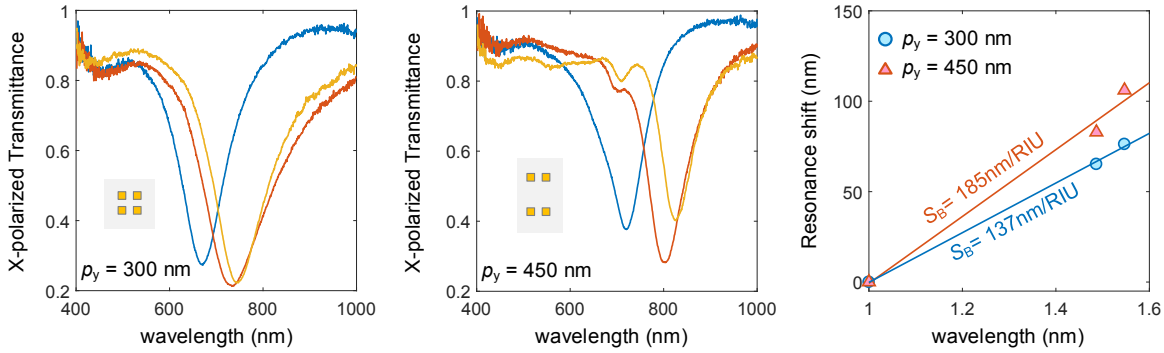

Figure S2. Bulk sensing performance of rectangular plasmonic disk array with p_y = 300 nm (equivalent to the "Array 1" or background resonance) and p_y = 450 nm (equivalent to the "Array 2", for the lattice resonance) for a fixed x-periodicity p_x = 200 nm. The samples were coated by different e-beam resists, namely PMMA (n_{cl} = 1.4867) and ZEP (n_{cl} = 1.5468).

Table S1. Bulk sensing parameters of disk arrays (with p_x, p_y based on Fig. 4).

Parameters	Array 1	Array 2
Bulk sensitivity (S_B) (nm/RIU)	137	185
FWHM (nm)	103.4	99.9
Q-factor	6.48	7.22
Figure of Merit (FoM) (RIU^{-1})	1.33	1.85
Mode position (nm)	670.3	720.9

Table S2. Comparison between the proposed 3-disk structure with other structures employing different sensing mechanisms, resonance mechanisms, mode excitation, and fabrication methods.

Structures	Working principles	Mode excitation	Fabrication method	Sensing parameters	References	Remarks
Elliptical nanohole arrays	Differential polarization spectra	Normal incidence	Nanosphere lithography	$FoM \sim 151$ $S_B \sim 301 nm/RIU$ $\Delta\lambda \sim 2nm$ $\lambda_R \sim 1000nm$	Nanoscale 2017, 9, 14710	-Based on silver (Ag) -Sensing performance based on ΔT^{-1}
Nanoslit and nanocrevices	Surface Plasmon Polariton	Oblique incidence	Nanosphere lithography	$FoM \sim 730$ $S_B \sim 5833 nm/RIU$ $\Delta\lambda \sim 3 - 8nm$ $\lambda_R \sim 600 - 960nm$	Adv. Mater. 2018, 30, 1706031	SPP-based sensing
Nanodisk array	Surface lattice resonances	Normal incidence	Top-down: EBL, Ion Milling	$FoM \sim 25$ $\Delta\lambda \sim 18nm$ $S_B \sim 440nm$ $\lambda_R \sim 730 - 760nm$	ACS Nano 2011, 5, 5151	-Symmetrical cladding -Uniform periodicity
Gold mushroom arrays	Mode hybridization between top and bottom structures	Oblique incidence	Interference lithography	$FoM \sim 108$ $S_B \sim 1015 nm/RIU$ $\Delta\lambda \sim 9.5nm$ $\lambda_R \sim 1240 - 1350nm$	Nat. Commun. 2013, 4, 2381	Photoresist as the spacer between the top and bottom structures
3-disk array	Hybridization of surface lattice resonances	Normal incidence	Top-down: EBL, lift-off	$FoM \sim 24$ $S_B \sim 200 - 240 nm/RIU$ $\Delta\lambda \sim 6 - 10nm$ $\lambda_R \sim 750 - 850nm$	This work	Asymmetrical cladding (air cladded)

3. Spectral variation of measured plasmonic antenna

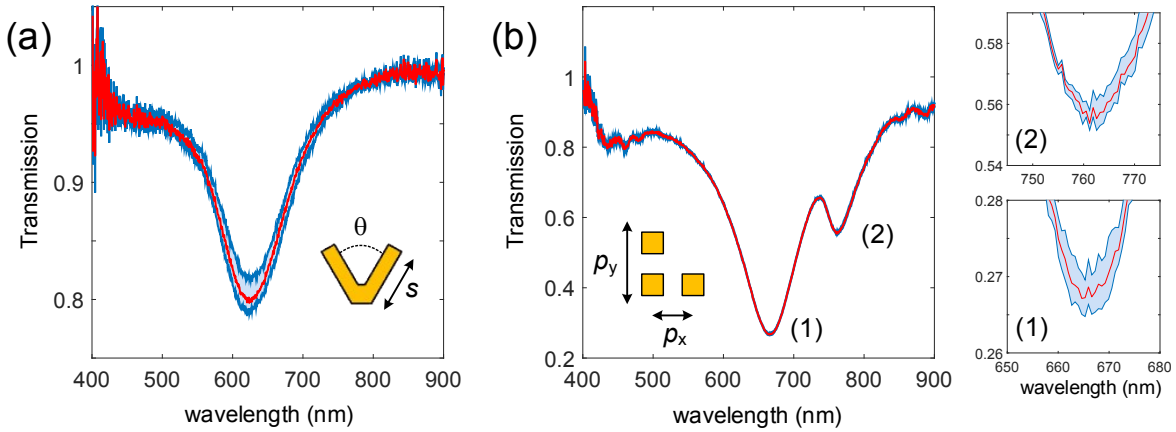

Figure S3. Spectral variation of plasmonic nanoantenna. (a) *v*-shaped split ring resonator (*v*-SRR), with θ = 60 nm and s = 60 nm. (b) 3-disk arrays with p_x = 200 nm, p_y = 450 nm, and s = 100 nm. The zoomed-in of the spectral variations at the background and narrow resonances are shown in Inset (1) and (2), respectively.

4. Standard deviation of plasmonic mode position as a function of resonance Q factor.

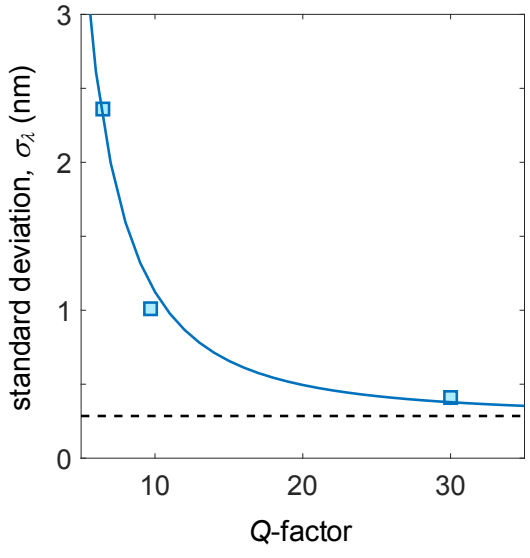

Figure S4. Standard deviation σ_λ for the resonance positions as a function of resonance Q-factor, which can be empirically fitted by $\sigma_\lambda(Q) = 83.83/Q^2 + 0.29$. The flat dashed line denotes the measurement error due to wavelength sampling of the equipment.

Table S2. Resonance shift of 3-disk arrays coated with alkanethiols.

Carbon length	Resonance shift (nm)		Remarks
	p_y = 450 nm	p_y = 500 nm	
0	0	0	uncoated
14	4.35	2.31	short-chain effect
16	12.46	12.69	monolayer
18	21.77	17.31	monolayer

5. Surface sensitivity and plasmonic decay length characteristics of 3-disk structure.

Measured resonance shifts for different carbon chains is shown in Table S2. The resonance shift for different coating thickness is shown in Fig. S5. The gold permittivity is taken from experimental values from gold thin film (D. I. Yakubovsky, A. V. Arsenin, Y. V. Stebunov, D. Yu. Fedyanin, V. S. Volkov. Optical constants and structural properties of thin gold films, *Opt. Express* **25**, 25574-25587 (2017)), while the substrate is chosen to the SiO_2. The simulated data is fitted with $\Delta\lambda_R(t) = S_B^{(sim)}\Delta n_a[1 - exp(-2t/L_d)]$, where $S_B^{(sim)} = \Delta\lambda_R(t\to\infty)/\Delta n_a = 347nm/RIU$ is the simulated bulk sensitivity obtained from the asymptote for the resonance shift, and $L_d = 36.53nm$ is the decay length of the plasmonic field. Experimentally, the decay length is likely the same as that in the simulation. The fitting is then changed by incorporating the experimentally obtained bulk sensitivity, i.e., $\Delta\lambda_R(t) = S_B^{(exp)}\Delta n_a[1 - exp(-2t/L_d)]$, with $0.4 < \Delta n_a < 0.5$ range is used to estimate the range of alkanethiol thickness.

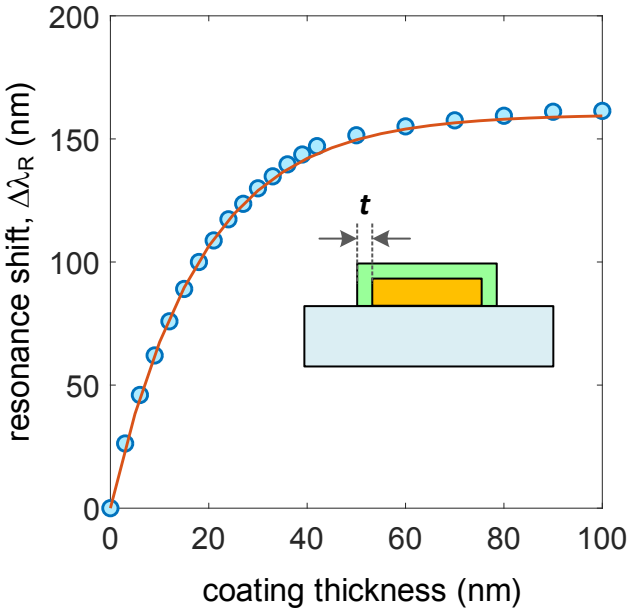

Figure S5. Simulated resonance shift of 3-disk arrays coated with dielectric shell of $n_a = 1.462$. The periodicities are $(p_x,p_y) = (200nm,450nm)$ and the size is $s_x = s_y = 100nm$.

6. Spectral mapping of 3-disk structure in different dielectric environments.

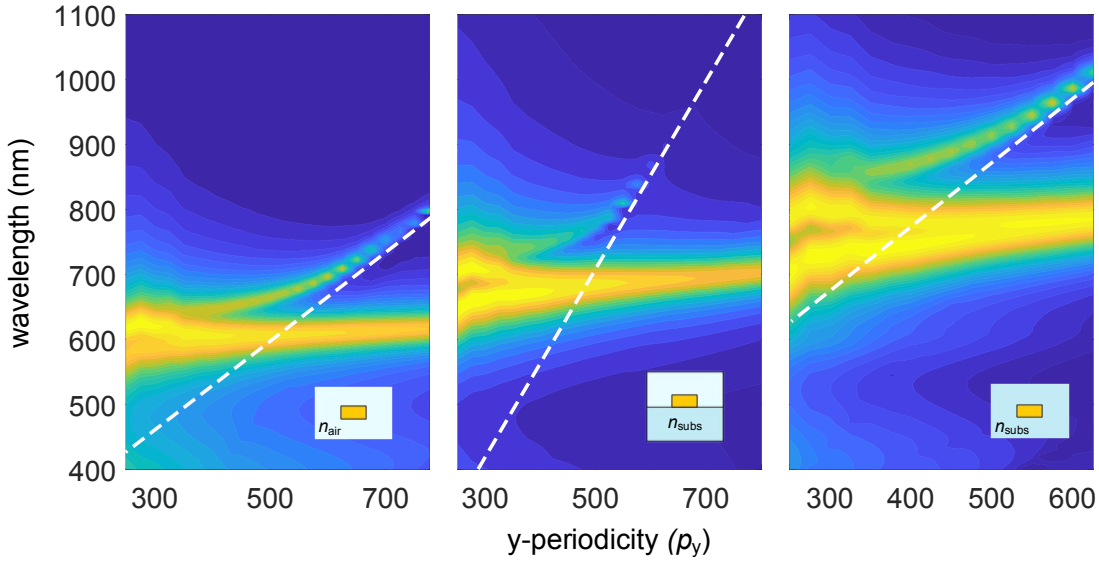

Fig. S6. The mapping of 3-disk structure in 3 dielectric environments: (a) air, (b) glass substrate, and (c) inside dielectric medium. The lattice modes in all cases are indicated by the dashed linear lines. With more symmetric environments, a stronger spectral contrast is observed.